第 48 卷 第 20 期/2021 年 10 月/中国激光 研究论文

中国激光

基于受激拉曼散射的高效率、大能量 1197 nm 激光器

房春奇[1,2]，于广礼[2]，丁建永[1,2]，李彬彬[2]，李高龙[2]，周军[2]，朱小磊[3]，韦玮[1*]

[1]南京邮电大学电子与光学工程学院，微电子学院，江苏 南京 210046；

[2]南京先进激光技术研究院先进全固态激光技术研发中心，江苏 南京 210046；

[3]中国科学院上海光学精密机械研究所，上海 201800

摘要 随着医学光声成像和荧光探测技术的迅速发展，波长为 1197 nm 的激光光源，特别是拉曼激光器受到了人们的关注。但目前 1197 nm 拉曼激光器存在的主要问题是输出能量低、稳定性较差等。为此提出了一种结构紧凑、高效率、大能量拉曼激光器的设计方案和原型样机制备。当 300 mJ 的 1064 nm 激光注入到腔外的硝酸钡晶体时，可获得能量为 137 mJ、脉宽为 7.4 ns 的 1197 nm 激光输出，拉曼转换效率最高达到 46.6%，1 h 内能量稳定度为 0.48%。该样机的输出特性优良，已成功用于医学光声成像，具备良好的产业化前景。

关键词 激光器；固体激光器；受激拉曼散射；$Ba(NO_3)_2$ 晶体；高效率

中图分类号 TN248.1 **文献标志码** A **doi**：10.3788/CJL202148.2001001

1 引 言

1197 nm 激光处于 C-H 键的光声成像窗口，可用于肿瘤、脂肪等生物组织的临床诊断及治疗，其倍频后的黄光波段在荧光探测领域也有着广泛的应用[1-4]。因此，对 1197 nm 激光器进行研究，提高其输出性能和可靠性，使其满足工程化应用具有十分重要的意义。然而，目前尚未发现可直接产生 1197 m 激光的增益介质，只能考虑利用非线性频率变换技术获得，如倍频、受激拉曼散射(SRS)等。但由于缺乏相应的基频光难以倍频，受激拉曼散射便成为了产生该波段激光的主要方式，其中采用晶体作为拉曼介质的固体激光器体积小、增益高，已成为当前的研究热点。

目前，使用比较广泛的拉曼晶体主要有硝酸钡[$Ba(NO_3)_2$][5-8]、钨酸盐[9-11]和钒酸盐[12]等晶体。其中 $Ba(NO_3)_2$ 具有最大的稳态拉曼增益，达到了 11 cm/GW@1064 nm，被称为纳秒激光器的首选拉曼晶体。更重要的是，$Ba(NO_3)_2$ 的拉曼频移为 1047.3 cm^{-1}，可将 1064 nm 激光移频到 1197 nm，而其他晶体由于频移较小不能达到该波段。因此，$Ba(NO_3)_2$ 非常适合作为 1197 nm 激光器的拉曼介质。2007 年，陈慧挺等[13]报道了一种外腔式拉曼激光器，利用 $Ba(NO_3)_2$ 晶体频移产生 1198.5 nm 激光，光光效率为 32.9%。2012 年，Agnesi 等[14]研究了 $Ba(NO_3)_2$ 在亚纳秒激光泵浦下的拉曼特性，获得了 150 ps 的窄脉冲激光，但能量只有 116 μJ。2013 年，Li 等[15]同样采用外腔式拉曼的结构产生了 21.4 mJ 的 1197 nm 激光，转换效率提升至 34.8%，并成功对肌内脂肪实现三维光声成像，验证了 1197 nm 激光器的应用价值。

为了进一步提高 1197 nm 激光器的效率和输出能量，本文研究了一种采用 1064 nm 激光泵浦 $Ba(NO_3)_2$ 晶体的固体激光器，通过对基频光、拉曼谐振腔的优化，提升了输出能量和转换效率，最终获得能量 137 mJ、转换效率最高 46.6%的 1197 nm 激光输出。实验中 Nd:YAG 脉冲激光器采用了高斯输出镜，使得 1064 nm 光束近似呈平顶分布，可在拉曼晶体中获得比较均匀的增益。为了提高基频光在拉曼晶体中的峰值功率密度，使用光束整形系统对基频光进行了缩束。此外，对拉曼谐振腔输出镜的选择性镀膜有效抑制了高阶斯托克斯光振荡，

收稿日期：2020-12-31；**修回日期**：2021-02-19；**录用日期**：2021-03-16

基金项目：江苏省研究生科研与实践创新计划项目(SJCX19_0277，KYCX19_0926)

通信作者：*weiwei@njupt.edu.cn

基频光与一阶斯托克斯光之间转换效率大大提高。该激光器效率高、输出能量大，能量稳定性也达到了工程化应用水平，在生物医学领域具有广泛的应用前景。

2　实验装置

2.1　拉曼激光器结构设计与装置

1197 nm 拉曼激光器的结构原理如图 1 所示，其中，M1～OC1 为 1064 nm 基频光谐振腔，M2～QWP2 为光隔离与光束整形模块，M4～OC2 为 1197 nm 拉曼谐振腔。

1064 nm 谐振腔采用氙灯侧面泵浦 Nd∶YAG 晶体[Φ7 mm×105 mm，掺杂原子数分数(1±0.1)%，高透(AR)1064 nm]，通过水循环系统进行冷却，控温 25 ℃。M1[高反(HR)1064 nm，R=2 m]为平凹镜，OC1(T=70%@1064 nm，R=1 m)为高斯变反射率输出镜，可使输出激光由高斯光束转变为近平顶光束。同时，腔内插入偏振片、λ/4 波片、KD*P 调 Q 模块(Φ25.4 mm×39 mm，AR1064 nm)形成窄脉冲输出。45°反射镜 M2、M3(HR1064 nm)使激光器形成 U 型光路，提高系统紧凑性。半波片 HWP1、HWP2、偏振分光棱镜 PBS1、PBS2 与法拉第旋光器组合形成光隔离器，防止产生返回光。透镜组 L1(f=70 mm，AR1064 nm)和 L2(f=−50 mm，AR1064 nm)对光束进行整形、缩束，提高基频光在 $Ba(NO_3)_2$ 晶体中的峰值功率密度。

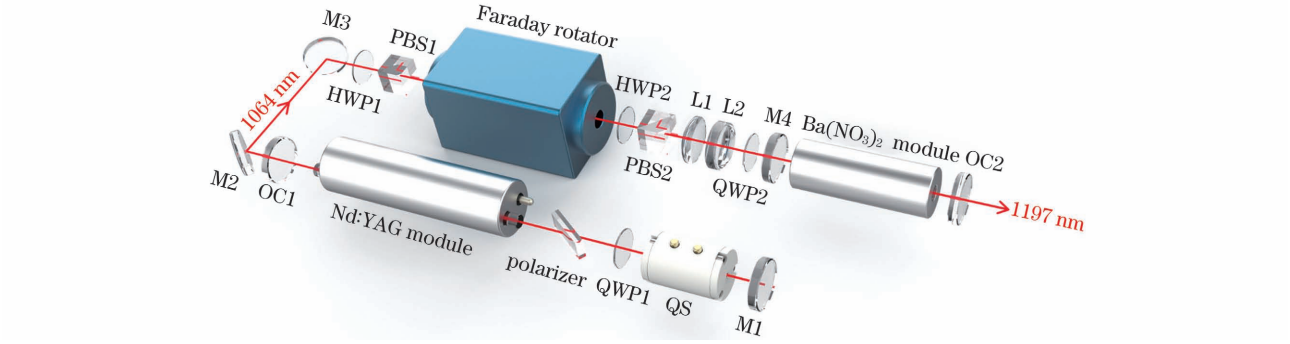

图 1　激光器装置结构原理示意图

Fig. 1　Structural schematic of laser device

内腔式拉曼激光器很容易产生受激布里渊散射、自聚焦等非线性效应，影响一阶斯托克斯光转换效率，因此本文采用了外腔式拉曼谐振腔结构。对外腔式固体拉曼激光器进行了建模仿真和数值优化[16]，若已知激光器的归一化拉曼增益系数 G_L 和归一化泵浦脉宽 N_L，即可推导出拉曼谐振腔的最佳反射率和最高转换效率。其中，G_L 和 N_L 用公式分别表示为

$$G_L = g_L I_{Lmax} l_R, \tag{1}$$

$$N_L = \frac{t_L \cdot c}{2l}, \tag{2}$$

式中：g_L=11 cm/GW 为拉曼增益系数；I_{Lmax} 为基频光功率密度；l_R 为拉曼晶体长度；t_L 为基频光脉宽；c 为光速；l 为拉曼谐振腔腔长。将 I_{Lmax}=150 MW/cm^2、l_R=30 mm、t_L=10 ns 和 l=110 mm 代入(1)式和(2)式可得 G_L=4.95，N_L=13.6，查阅文献[16]可知，相应的最佳反射率 $R_{opt}\approx$55%，最高转换效率 $\eta_{max}\approx$52%，一阶斯托克斯光起振阈值 $I_{th}\approx$50 MW/cm^2。因此，本文中拉曼谐振腔输出镜拟采用 45%透过率的透镜。拉曼谐振腔腔镜由 M4 和 OC2 组成，腔长约 110 mm。腔镜 M4(AR1064 nm&HR1197 nm)为平平镜，对基频光高透并且对一阶斯托克斯光高反。拉曼晶体为 $Ba(NO_3)_2$(8 mm×8 mm×30 mm，AR1064 nm&1197 nm)，为了解决该晶体易潮解的特性，需对其进行封装处理，封装后实物如图 2 所示。OC2(T=45%@1197 nm，HR1064 nm&AR1369 nm)对 1197 nm 激光透过率为 45%形成拉曼光输出，镀 1369 nm 增透膜以抑制高阶斯托克斯光起振，同时对 1064 nm 激光高反，实现双程泵浦，提高了 1064 nm 激光的利用效率。双程泵浦后剩余的基频光共经过 λ/4 波片 QWP2 两次，相位改变了 λ/2，接着由 PBS2 反射至腔外，被光阱吸收。

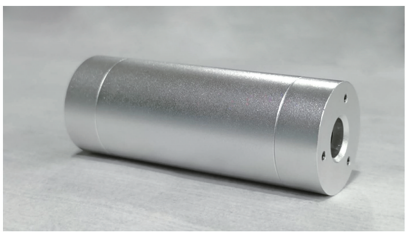

图 2　硝酸钡晶体模块结构图

Fig. 2　Structural schematic of $Ba(NO_3)_2$ module

2.2　性能测试与表征

本文中采用的波长测量仪器为美国海洋光学波长计(HR4000,Ocean Insight,美国)和日本横河光谱分析仪(AQ6370C,YOKOGAWA,日本);脉冲宽度由高速光电二极管(DET10A,Thorlabs,美国)测量,其波形通过带宽 500 MHz 的示波器(MDO3054,Tektronix,美国)表征;激光的输出能量及稳定性利用能量计(PE25-C,Ophir,以色列)记录。本实验所有性能测试均为在室温条件(25 ℃)下进行。

3　结果与讨论

根据图 1 搭建了 1064 nm 基频光谐振腔,设置氙灯参数为重复频率为 10 Hz、泵浦脉宽为 220 μs。首先在三种不同谐振腔长条件下,测量了 1064 nm 激光输出能量与氙灯电压之间的关系。如图 3(a)所示,三者输出能量随着电压提高而增加,其中腔长 305 mm 的能量相对较高,在电压 700 V 时可达 334 mJ,使用波长计测量其输出波长为 1064.3 nm[如图 3(a)插图所示]。选定 305 mm 为基频光谐振腔最终腔长,测量输出能量 334 mJ 时的脉冲波形,如图 3(b)所示,脉宽宽度约 10.5 ns。利用感光相纸记录输出镜处的光斑图形,如图 3(b)插图所示,在高斯输出镜作用下,光斑较为均匀,近似平顶分布。使用透镜变换法,测得能量 334 mJ 时激光光束发散全角为 1.1 mrad。

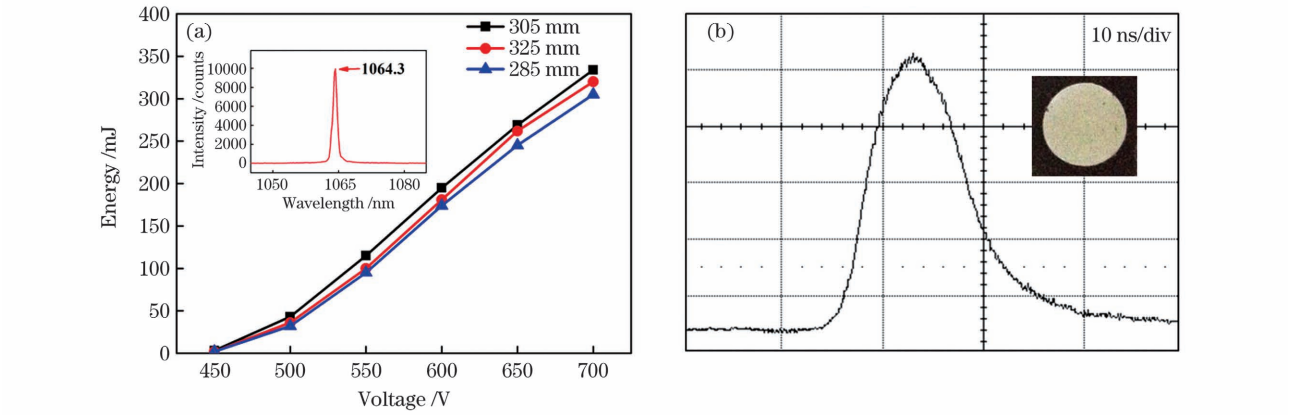

图 3　1064 nm 激光输出特性。(a)不同腔长条件下的输出能量(插图:最大输出能量时的波长);(b)脉冲宽度(插图:光斑分布)

Fig. 3　Output characteristics of 1064 nm laser. (a) Output energy at different cavity lengths (inset: wavelength of laser at the maximum output energy); (b) pulse width (inset: beam image)

由于 1064 nm 激光呈发散趋势,且光斑较大,需要利用透镜组对基频光进行缩束。测得缩束后硝酸钡晶体处的光斑直径为 5 mm,计算能量 300 mJ 时基频光峰值功率密度约 145.5 MW/cm^2。为了确定 1197 nm 谐振腔输出镜最佳透过率,选择了三种不同透过率的输出镜(T=35%、40%、45%)进行了实验,输出能量与泵浦能量的关系如图 4(a)所示,图 4(b)是相应的转换效率。由图 4 可知,透过

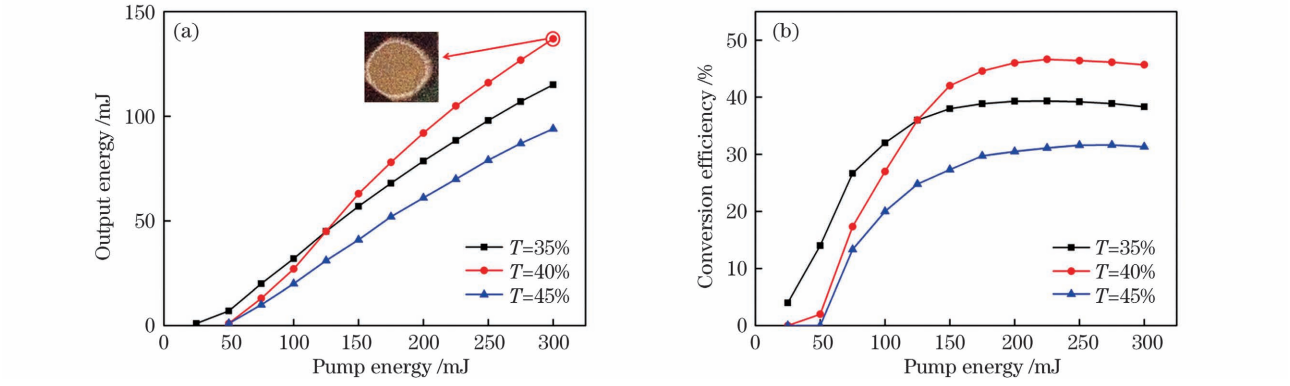

图 4　1197 nm 激光输出特性。(a)不同输出镜透过率时 1197 nm 输出能量(插图:能量 137 mJ 时的光斑);(b)1197 nm 转换效率

Fig. 4　Output characteristics of 1197 nm laser. (a) Output energy of 1197 nm laser at different output mirror transmittance(inset: beam image at 137 mJ); (b) conversion efficiency of 1197 nm laser

率 $T=40\%$可以获得最大输出能量，与理论计算的最佳反射率 $R_{opt}\approx55\%$大致相同。$T=40\%$时，一阶斯托克斯光在 24.3 MW/cm^2 时起振，小于理论值，这是由于 $I_{th}\approx50$ MW/cm^2 是按照单程泵浦计算的结果，而实验中采用的是双程泵浦。随着泵浦能量的增加，1197 nm 能量最大达到 137 mJ，此时光斑如图 4(a)插图所示，由于缩束、热效应等因素影响，光斑略微变形，但分布仍较为均匀，测量其发散全角约 5 mrad。

从图 4(b)可以发现，转换效率先随着泵浦能量提高而大幅增加，之后趋于平缓甚至略微下降，分析可能有两个原因，一是转换效率饱和后泵浦能量达到了二阶斯托克斯光的起振阈值，部分一阶斯托克斯光转换为二阶斯托克斯光，导致效率降低；二是由于大能量泵浦时 $Ba(NO_3)_2$ 晶体的热效应越来越严重，影响了谐振腔的稳定性，使得效率降低。使用色散棱镜发现激光可分成两束，测量较弱的一束激光能量约 2 mJ，波长 1369.61 nm，说明的确产生了高阶斯托克斯光。三种透过率的输出镜中，$T=40\%$时激光器具有最高的拉曼转换效率，在泵浦能量 225 mJ 时最大，此时 1197 nm 输出能量 105 mJ，转换效率 46.6%，与理论值较为吻合，但因晶体材料、膜层参数、测量误差等影响与理论值存在一定偏差。

采用横河光谱仪测得输出能量 137 mJ 时激光的波长为 1197.81 nm，如图 5(a)所示。图 5(b)为 1197 nm 激光的脉冲波形，脉宽从 10.5 ns 压缩到了 7.4 ns。

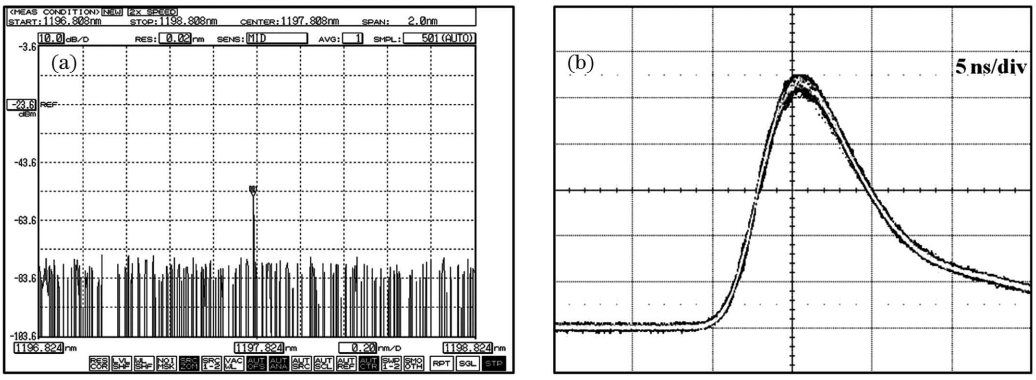

图 5　1197 nm 激光的输出特性。(a)波长；(b)脉宽

Fig. 5　Output characteristic of 1197 nm laser. (a) Wavelength; (b) pulse width

最后，测量了激光器 1 h 内的能量稳定性，能量不稳定度(RMS)为 0.48%，如图 6(a)所示。由此可见，该激光器的指标参数和稳定性都达到了工程化的水平，性能优良，据此设计并开发了一台 1197 nm 拉曼激光器工程样机，外观如图 6(b)所示。

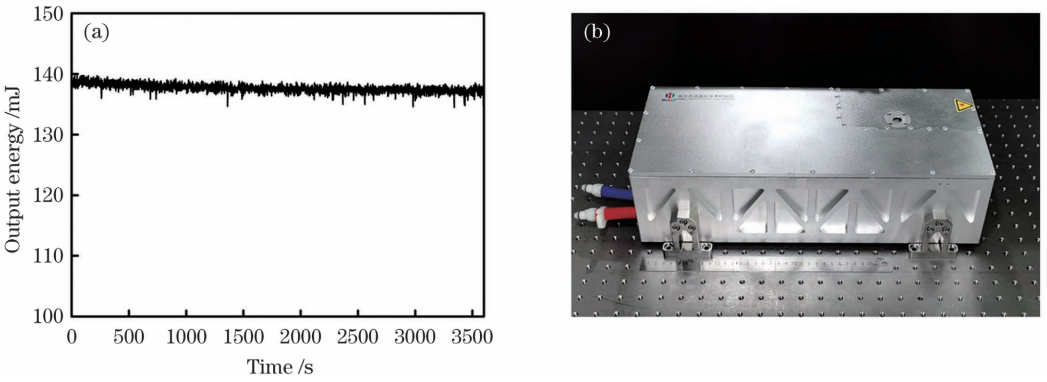

图 6　激光器能量稳定性与实物图。(a)1 h 内的能量稳定性；(b)外观图

Fig. 6　Energy stability and picture of laser. (a) Energy stability within 1 h; (b) picture

4　结　　论

本文研究了一种基于外腔受激拉曼散射的固体激光技术，制备了一台高效率、大能量 1197 nm 脉冲激光器。通过改变谐振腔长、采用高斯输出镜等措施，优化了基频光的能量和光斑分布，最高可输出

334 mJ 的 1064 nm 激光，此时脉宽为 10.5 ns。利用透镜组对基频光束进行了缩束，增大峰值功率密度，提高了拉曼转换效率。同时，对拉曼腔镜选择性镀膜抑制高阶斯托克斯光起振，增大了一阶斯托克斯光的输出能量，最终获得了 137 mJ 的 1197 nm 激光输出，脉宽为 7.4 ns，拉曼转换效率最大为 46.6%，1 h 内能量稳定性(RMS)为 0.48%。该系统输出能量和转换效率高，能量稳定性好，成本低，可为光声成像、荧光探测等应用提供优质光源，具有广泛的应用前景。

参 考 文 献

[1] Rajian J R, Li R, Wang P, et al. Vibrational photoacoustic tomography: chemical imaging beyond the ballistic regime [J]. The Journal of Physical Chemistry Letters, 2013, 4(19): 3211-3215.

[2] Shilova G V, Sirotkin A A, Zverev P G. Diode pumped Nd^{3+}:YVO_4 laser with intracavity SHG in LBO and SRS in $Ba(NO_3)_2$ [C]//2018 International Conference Laser Optics (ICLO), June 4-8, 2018, St. Petersburg, Russia. New York: IEEE Press, 2018: 37.

[3] Chu H, Zhang Z Y, Wang S H, et al. Efficient all solid-state continuous-wave orange laser at 598 nm [J]. Laser Physics, 2011, 21(7): 1180-1183.

[4] Zhao H, Wang H Y, Zhu S Q, et al. 578.5 nm end-pumped passively *Q*-switched Raman yellow laser [J]. Laser & Optoelectronics Progress, 2021, 58(1): 0114004.
赵辉, 王浩宇, 朱思祁, 等. 578.5 nm 端面泵浦被动调 *Q* 拉曼黄光激光器[J]. 激光与光电子学进展, 2021, 58(1): 0114004.

[5] Shilova G V, Zverev P G, Sirotkin A A. Diode pumped Nd:YVO_4/LBO/$Ba(NO_3)_2$ Raman laser at 563 nm [J]. Laser Physics Letters, 2020, 17(6): 065801.

[6] Chen J C, Zou X, Peng Y J, et al. 1.88 μm, $Ba(NO_3)_2$-based Raman laser pumped by a potassium-titanyl-phosphate-based optical parametric oscillator laser [J]. Chinese Optics Letters, 2016, 14(11): 75-78.

[7] Wang X B, Niu X, Wang X L, et al. An eye-safe extra cavity Raman laser in 1.5 μm with a $Ba(NO_3)_2$ crystal[J]. Applied Laser, 2016, 36(2): 211-214.
王旭葆, 牛霞, 王小磊, 等. 1.5 μm 外腔式 $Ba(NO_3)_2$ 人眼安全拉曼激光器[J]. 应用激光, 2016, 36(2): 211-214.

[8] Pask H M, Myers S, Piper J A, et al. High average power, all-solid-state external resonator Raman laser [J]. Optics Letters, 2003, 28(6): 435-437.

[9] Ren X K, Xie J, Ruan S C, et al. First-stokes Raman lasers based on $ZnWO_4$/Nd:YAG [J]. Chinese Journal of Lasers, 2020, 47(6): 0601003.
任席奎, 谢建, 阮双琛, 等. 基于 $ZnWO_4$/Nd:YAG 的一阶斯托克斯拉曼激光器[J]. 中国激光, 2020, 47(6): 0601003.

[10] Sheintop U, Sebbag D, Komm P, et al. Two-wavelength Tm: YLF/KGW external-cavity Raman laser at 2197 nm and 2263 nm[J]. Optics Express, 2019, 27(12): 17112-17121.

[11] Wetter N U, Ferreira M S, Pask H M. Intracavity diode-side-pumped Raman laser at 1147 nm and 1163 nm[J]. Proceedings of SPIE, 2018, 10518: 1051816.

[12] Cheng M Y, Duan Y M, Sun Y L, et al. Research progress of Raman and frequency mixing for visible lasers based on vanadate crystals [J]. Laser & Optoelectronics Progress, 2020, 57(7): 071611.
程梦瑶, 段延敏, 孙瑛璐, 等. 钒酸盐晶体拉曼及其混频可见光波段激光研究进展[J]. 激光与光电子学进展, 2020, 57(7): 071611.

[13] Chen H T, Lou Q H, Dong J X, et al. High efficiency, short-pulse 1198.5 nm $Ba(NO_3)_2$ Raman laser[J]. Acta Photonica Sinica, 2007, 36(4): 581-584.
陈慧挺, 楼祺洪, 董景星, 等. 高效率, 窄脉冲 1198.5 nm $Ba(NO_3)_2$ 喇曼激光器[J]. 光子学报, 2007, 36(4): 581-584.

[14] Agnesi A, Caracciolo E, Carrà L, et al. 150-ps pulse Raman generator pumped by a 1-kHz sub-nanosecond passively *Q*-switched laser system [J]. Applied Physics B, 2012, 107(3): 691-695.

[15] Li R, Slipchenko M N, Wang P, et al. Compact high power barium nitrite crystal-based Raman laser at 1197 nm for photoacoustic imaging of fat[J]. Journal of Biomedical Optics, 2013, 18(4): 040502.

[16] Ding S H. Theoretical and experimental research on all solid state Raman laser [D]. Jinan: Shandong University, 2006: 37-47.
丁双红. 全固态拉曼激光器理论与实验研究[D]. 济南: 山东大学, 2006: 37-47.

High-Efficiency and High-Pulse-Energy 1197 nm Laser Based on Stimulated Raman Scattering

Fang Chunqi[1,2], Yu Guangli[2], Ding Jianyong[1,2], Li Binbin[2], Li Gaolong[2], Zhou Jun[2], Zhu Xiaolei[3], Wei Wei[1*]

[1] *College of Electronic and Optical Engineering, College of Microelectronics, Nanjing University of Posts and Telecommunications, Nanjing, Jiangsu* 210046, *China*;

[2] *Advanced All Solid State Laser Technology R&D Center, Nanjing Institute of Advanced Laser Technology, Nanjing, Jiangsu* 210046, *China*;

[3] *Shanghai Institute of Optics and Fine Mechanics, Chinese Academy of Sciences, Shanghai*, 201800, *China*

Abstract

Objective The 1197 nm laser is located in the photoacoustic imaging window of the C–H bond, which can be used for the clinical diagnosis and treatment of biological tissues, such as tumors and fats. Additionally, its frequency-doubled yellow light has a wide range of applications in the field of fluorescence detection. However, the 1197 nm Raman laser suffers from low energy and poor reliability, making it unsuitable for engineering applications. In this paper, we conducted experiments to investigate the ways to improve the energy and efficiency of the 1197 nm Raman laser. On the one hand, the beam distribution and energy of fundamental light were improved to demonstrate their effect on Raman efficiency. On the other hand, the Raman laser was optimized theoretically and experimentally. A high-efficiency and high-energy solid-state Raman laser is studied and a prototype of this laser is developed to test its performance.

Methods In this study, we investigated an external resonator stimulated by Raman scattering technology and demonstrated a $Ba(NO_3)_2$ Raman laser pumped by a Q-switched 1064 nm laser. First, a xenon-lamp-pumped Nd∶YAG laser was constructed. Experiments were conducted using three different cavity length conditions to determine the best cavity length of the resonator and simultaneously increase the output energy. To improve the uniformity of the 1064 nm beam, the laser output coupler adopted a variable reflectivity output mirror. Then, the beam diameter of the Nd∶YAG laser was compressed to 5 mm using a 1.5× telescope to increase the peak power density of the fundamental light. Thereafter, we optimized the parameters of the external-resonator Raman laser according to the rate equation and radiation transmission theories, such as the optimum reflectivity, the threshold of first-order Stokes light, and the highest conversion efficiency. Moreover, the output coupler of the Raman laser was selectively coated to suppress the oscillation of high-order Stokes light. Then, the external-cavity Raman laser experiment was performed and the differences between the experimental results and theoretical values were compared. Finally, a prototype of a 1197 nm Raman laser was built to verify its reliability and stability.

Results and Discussions The experimental results of the 1064 nm and 1197 nm resonators are shown in this study. Figure 3(a) shows that 305 mm is the best cavity length under the three cavity length conditions. The maximum output energy, wavelength, and pulse width are 334 mJ, 1064.3 nm, and 10.5 ns, respectively. When the variable reflectivity output coupler is used, the 1064 nm beam is uniform with a flat top distribution [Fig. 3(b)] and the divergence angle is 1.1 mrad. The fundamental beam passed through a 1.5× telescope, and its peak power density was increased to 145.5 MW/cm^2. According to theoretical calculations of the external-resonator Raman laser, the best reflectivity of the output coupler is 55% and the highest conversion efficiency is 52%. Figures 4 and 5 show the output characteristics of the 1197 nm Raman laser. The best transmittance of the output coupler is 40%, which is consistent with the theory. When a 300 mJ 1064 nm laser was injected into the barium nitrate crystal, a steady laser at 1197.81 nm with an output energy of 135 mJ, a pulse width of 7.4 ns, and a divergence angle of 5 mrad was obtained. The maximum conversion efficiency was 46.6%, which was slightly different from the theory. This is because the second-order Stokes light starts to oscillate, and the thermal effect of Raman crystal becomes more severe. A prototype of the 1197 nm Raman laser was developed, as shown in Fig. 6(b). The energy stability (RMS) within 1 h is 0.48% [Fig. 6(a)], indicating that both the output characteristics and reliability meet the requirements of engineering applications.

Conclusions We study the solid-state laser technology based on external-cavity stimulated Raman scattering and fabricate a high-efficiency and large energy 1197 nm pulse laser. By varying the resonant cavity length and using a variable reflectivity output coupler, the energy and beam distribution of the fundamental light are optimized. The maximum output wavelength of the 1064 nm laser is 334 mJ, and the pulse width is 10.5 ns. The fundamental beam is compressed by a 1.5× telescope to increase the peak power density and improve the Raman conversion efficiency. In addition, the selective coating on the output coupler suppresses the oscillation of high-order Stokes light, increasing the output energy of the first-order Stokes light. When the injected energy reaches 300 mJ, we obtained a 1197.81 nm laser of 137 mJ with a pulse width of 7.4 ns. The maximum Raman conversion efficiency is 46.6%, and the energy stability (RMS) within 1 h is 0.48%. Generally, the prototype of the 1197 nm Raman laser has been successfully used in medical photoacoustic imaging. The system has the advantages of high output energy and conversion efficiency, good energy stability, and low cost. It can provide high-quality light sources for photoacoustic imaging and fluorescence detection and has broad application prospects.

Key words lasers; solid-state laser; stimulated Raman scattering; $Ba(NO_3)_2$ crystal; high-efficiency

OCIS codes 140.3580; 190.5650; 140.3540